ELSEVIER

Cement & Concrete Composites 26 (2004) 113–126

Cement & Concrete Composites

www.elsevier.com/locate/cemconcomp

Thermal induced stress and associated cracking in cement-based composite at elevated temperatures—Part II: thermal cracking around multiple inclusions

Y.F. Fu [a], Y.L. Wong [a,*], C.A. Tang [b], C.S. Poon [a]

[a] Department of Civil and Structural Engineering, The Hong Kong Polytechnic University, Hong Kong
[b] Lab of Numerical Test of Material Failure, Northeastern University, Shenyang 110006, China

Accepted 25 April 2003

Abstract

A 2-D mesoscopic thermoelastic damage model is developed and used to study the thermal stress field and associated fracture in a cement-based composite with multiple circular or irregular inclusions subjected to elevated temperatures. It is found that the thermal stress field and the associated cracking are dominated by (i) the thermal mismatch between the matrix and the inclusions, (ii) the arrangement of the inclusions, and (iii) the heterogeneity and the shape of the inclusions. Thermal radical cracks firstly occur between two adjacent inclusions, which have the shortest distance apart or sharp corners when the coefficient of thermal expansion of the inclusions is greater than that of the matrix. The propagation of radical cracks in the matrix will be terminated by the presence of an inclusion with higher strength at the crack tip. The numerical findings are also used to discuss the thermal cracking histories of concretes with different aggregate grading arrangements.

Keywords: Thermal stress; Thermal induced cracking; Irregular inclusion; Numerical simulation; Heterogeneity

1. Introduction

When a cement-based composite material is subjected to elevated temperatures, the difference in thermal properties of the cementitious matrix and the aggregate inclusions induces thermal stresses and possibly cracking in the concrete. Previous investigations [1,2] showed that the greater the mismatch in the mechanical and thermal properties between the matrix and the inclusion, the more significant would be the reduction of strength, elasticity modulus, and durability of concrete. The deteriorations of these properties were mainly due to thermal induced cracking. Venecanin [1] experimentally studied the effects of thermal incompatibility of concrete components (TICC) by measuring their coefficients of thermal expansion (CTE), and the CTE heterogeneity of aggregate inclusions. The results showed that the thermal properties, such as CTE, thermal anisotropy and the residual strain after cyclic temperature changes, are related to the TICC. Kristensen and Hansen [3] supported to the Venecanin's view in their investigations of the thermal cracking of cement paste and concrete using ultrasonic pulse velocity techniques. Their experimental results indicated that cement paste and concrete could be damaged by internal cracking due to differential temperature between the core and the surface of specimen. Furthermore, based on fracture mechanics and micromechanics approaches, an analytical model [4] was proposed to study the reduction of elastic modulus with increasing temperature due to the mismatch in the CTE between mortar and aggregate, by assuming a uniform distribution of cracks. Recently, both analytical modeling and numerical simulation [5] were used to analyze residual thermal stresses and CTE in two-phase composites. It was found that the predicted CTE of a two-phase material was dependent on the Young's modulus ratio and the difference between the CTE of the two phase materials. If the intergranular phase had a greater CTE than that of the grain, the intergranular phase and the grain would be stressed in tension and hydrostatic compression, respectively. Although the studies on the thermal stress and the thermal crack have been

* Corresponding author. Tel.: +852-2766-6009; fax: + 852-2334-6389.
E-mail address: ceylwong@inet.polyu.edu.hk (Y.L. Wong).

0958-9465/$ - see front matter © 2003 Elsevier Ltd. All rights reserved.
doi:10.1016/S0958-9465(03)00087-8

conducted numerically and experimentally, numerical studies of the thermal cracking process—the initiation, propagation and linkage of cracks in concrete at elevated temperatures have not been reported.

Concrete is a highly heterogeneous material that can be quantified in three levels: macroscale, mesoscale and microscale [6,7]. The heterogeneity is one of the main reasons that cause the concentration stress and local failure [8,9]. Although at room temperature, the effects of heterogeneity on the fracture processes in concrete have been reported in literatures [6,7], these studies did not consider the effects of heterogeneity among the phase materials of concrete on the stress development and cracking process under high temperatures.

In Part I of this paper [11], a 2-D mesoscopic thermoelastic damage (MTED) model [11] was presented, and the thermal cracking around a single inclusion due to different CTE, strength properties, and heterogeneity were discussed. The developed model is adopted here to quantify/qualify the effects of the arrangement, shape (circular and irregular) and CTE of multi-inclusions on the thermal stresses and associated cracking in a cement-based composite. These findings are also used to discuss the thermal cracking histories of concretes with different aggregate grading arrangements.

2. Numerical specimens

Eight numerical square specimens with different thermal and geometrical properties (see Table 1 and Table 2) are presented here to simulate the thermal induced cracking process in the composite with multi-inclusions. α_i and α_m denote the CTEs of the inclusion and the matrix, respectively.

Specimens no. 1 and 2 have multi-single-sized circular inclusions and identical percentage of inclusion content (see Fig. 1a). They are set to investigate the influence of thermal mismatch on the thermal stress field, and their only variable is the CTE of the inclusions. Specimen no. 3 is similar to specimen no. 1 except the diameter or the content of the inclusions (see Fig. 1b). The inclusions contents of specimens no. 1 and 3 are 28.3% and 50.2% respectively. They are used to study the effect of the size of inclusions on the thermal stress field. Specimen no. 4 that has an inclusion content of 46%, is prepared to simulate the complex thermal stress field in a composite with multi-inclusions of different diameters (see Fig. 1c). Each component (matrix and inclusion) of specimens no. 1–4 is assumed to be homogeneous and isotropic, and consequently the homogeneity index h has a value of 300.

Specimens no. 5–7 (see Fig. 1d and e) are similar to the corresponding specimens no. 1–3, except the former ones have a relative high degree of heterogeneity ($h = 3$ in matrix and inclusions).

Table 1
Material properties of specimens no. 1–4

Parameter	Value	
	Matrix	Inclusion
Homogeneity index (h)	300	300
Mean elastic modulus (MPa)	60,000	100,000
Mean compressive strength (MPa)	200	300
Poisson ratio	0.25	0.20
Coefficient of thermal expansion (/°C)		
Specimen 1		1.1×10^{-5}
Specimen 2		0.9×10^{-5}
Specimen 3	1.0×10^{-5}	1.1×10^{-5}
Specimen 4		1.1×10^{-5}
Temperature increment (°C)	10	10
Tension cutoff	0.1	0.1
Frictional angle (°)	30	30
Dimension (mm)		
Specimen 1	100×100	Φ15
Specimen 2		Φ15
Specimen 3		Φ20
Specimen 4		Different diameters
Number of elements		
Specimen 1	200×200	1412
Specimen 2		1412
Specimen 3		2354
Specimen 4		Different diameters

Table 2
Material properties of specimens no. 5–8

Parameter	Value	
	Matrix	Inclusion
Homogeneity index	3	3
Mean elastic modulus (MPa)	60,000	100,000
Mean compressive strength (MPa)	200	300
Poisson ratio	0.25	0.20
Coefficient of thermal expansion (/°C)		
Specimen 5		1.1×10^{-5}
Specimen 6		0.9×10^{-5}
Specimen 7	1.0×10^{-5}	1.1×10^{-5}
Specimen 8		1.1×10^{-5}
Temperature increment (°C)	10	10
Tension cutoff	0.1	0.1
Frictional angle (°)	30	30
Dimension (mm)		
Specimen 5	100×100	Φ15
Specimen 6		Φ15
Specimen 7		Φ20
Specimen 8		Polygon
Number of elements		
Specimen 5	200×200	1412
Specimen 6		1412
Specimen 7		2354
Specimen 8		Polygon

Specimen no. 8 (see Fig. 1f) has a random arrangement of irregular inclusions with different sizes, and an inclusion content of 61%. It is designed to study the effects of irregular inclusions on thermal cracking. Its

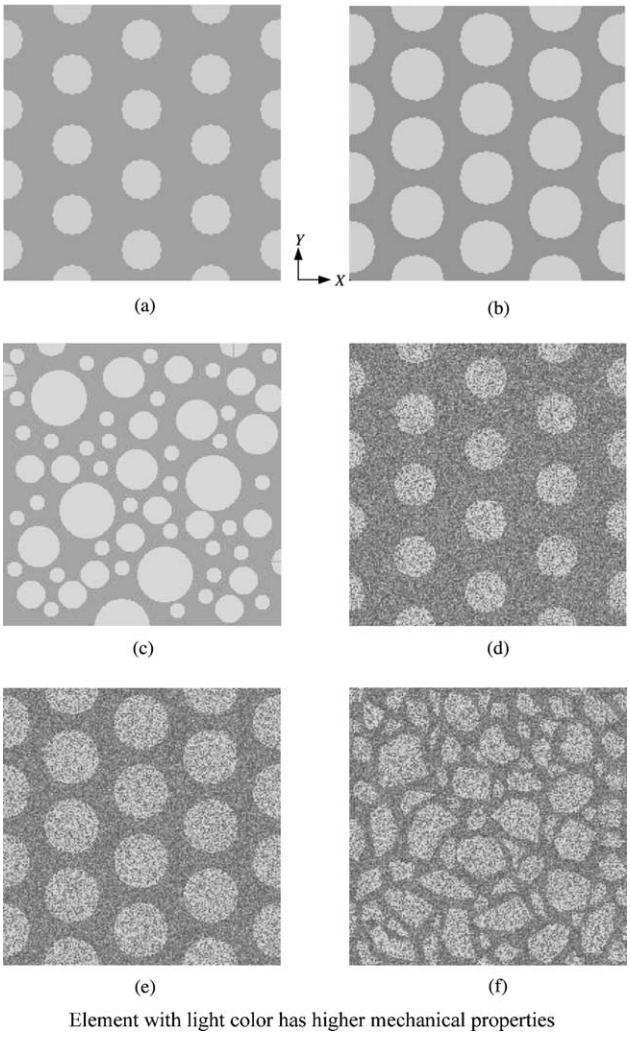

Fig. 1. Numerical specimens. (a) Specimens no. 1 and 2; (b) specimen no. 3; (c) specimen no. 4; (d) specimens no. 5 and 6; (e) specimen no. 7; (f) specimen no. 8.

mechanical and thermal properties are identical to those of specimen no. 4.

All specimens are subjected to uniform temperature field changes (steady state) ranging from 20 °C till 620 °C, at an increment of 10 °C, under a plain stress condition without any constraint on the boundaries.

3. Numerical simulation results and discussion

Fig. 2 shows the thermal stress fields of specimens no. 1 and 2. A comparison of the thermal stress fields between specimen no. 1 and 3 is shown in Fig. 3. The thermal stress fields of specimens no. 4 are presented in Fig. 4. For specimens no. 5–8, their thermal cracking processes are shown in Figs. 5–8, and their stress distributions along the mid-section *E–E* are plotted in Figs. 9–12. A detailed discussion of these figures is given below.

3.1. Thermal stress field

3.1.1. Effects of thermal mismatch

If the CTE of the inclusion is greater than that of the matrix, a hydrostatic compression is observed in the inclusions (see Fig. 2a and c), whereas a bi-axial stress state (compression and tension) is formed among the matrix (see Fig. 2c). If the CTE of the inclusion is less than that of the matrix, the inclusions are located in a tensile stress field (see Fig. 2b and d), whereas the zones among the inclusions are located in a bi-axial stress state (compression and tension). These observations are similar to those of single inclusion specimens presented in Part I of the paper [11].

3.1.2. Effects of arrangement of multi-inclusions

In the case of specimen no. 1 with multi-inclusions of 15 mm in diameter, a diamond-shaped region surrounded by the inclusions (see Fig. 2a) is chosen to discuss the influence of the arrangement of inclusions. In this region, the distance between the inclusions ***A*** and ***B*** is smaller than that between the inclusions ***C*** and ***D***. Consequently, in the sub-region Ψ_1, the stresses in the X-direction σ_x are smaller than 0 ($\sigma_x < 0$), and the stresses in the Y-direction σ_y are larger than 0 ($\sigma_y > O$). However, the sub-region Ψ_2 has $\sigma_x > 0$ and $\sigma_y < 0$ (as shown in Fig. 2c). In the locally enlarged pictures of the principal stress contours of the sub-regions Ψ_1 and Ψ_2 (see Fig. 2a), a dark line is a trajectory of a maximum principal stress and a light line is the trajectory of the minimum principal stress. It is evident that the values of all principal stresses approach zero in the sub-region Ψ_2, but the principal stresses in the sub-region Ψ_1 have the highest value in the whole matrix (see Fig. 2c). There are six sub-regions of low stress like Ψ_2 around each inclusion in the composite. Hence, the elements in Ψ_1 have higher probability of failure than those in Ψ_2.

Similar stress states in Ψ_1 and Ψ_2 are observed in specimen no. 3 with larger multi-inclusions of 20 mm diameter (see Fig. 3b and d). The calculated results are in good agreement with those reported in the literature [5,10]. They further confirm that the stress induced by the cross-effect of the inclusions is one of the reasons that causes the stress concentration. From Fig. 3c and d, it is found that the stresses between the inclusions ***A*** and ***B*** of specimen no. 3 are about 25% higher than those of specimen no. 1. Indeed, the stresses of specimen no. 3 are approximately 40% higher than those of the single inclusion situation reported in the companion paper [11]. Similar observations are found between the inclusions ***A*** and ***C***, or ***C*** and ***B***, or ***B*** and ***D***, or ***D*** and ***A***.

Consequently, the stress concentration in the matrix due to the cross-effect of multi-inclusions makes the elements in the matrix more prone to failure.

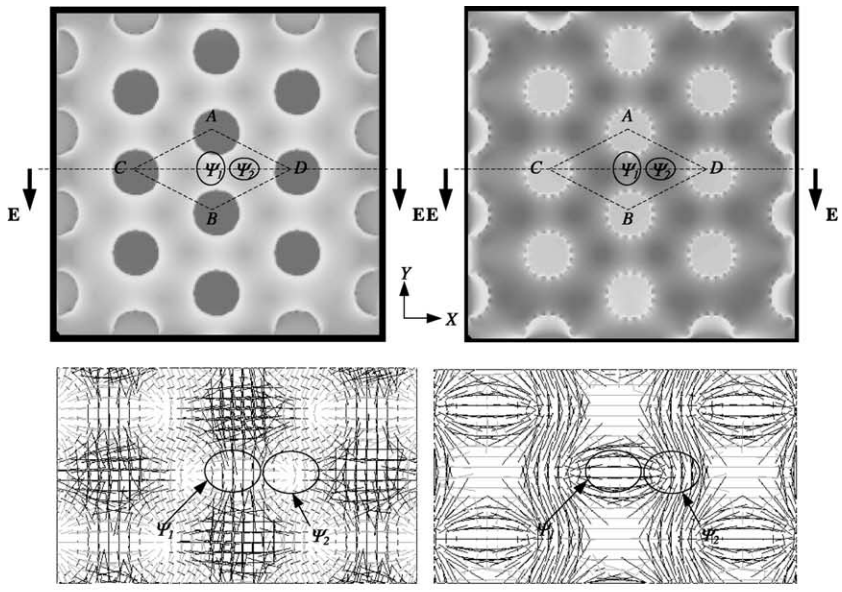

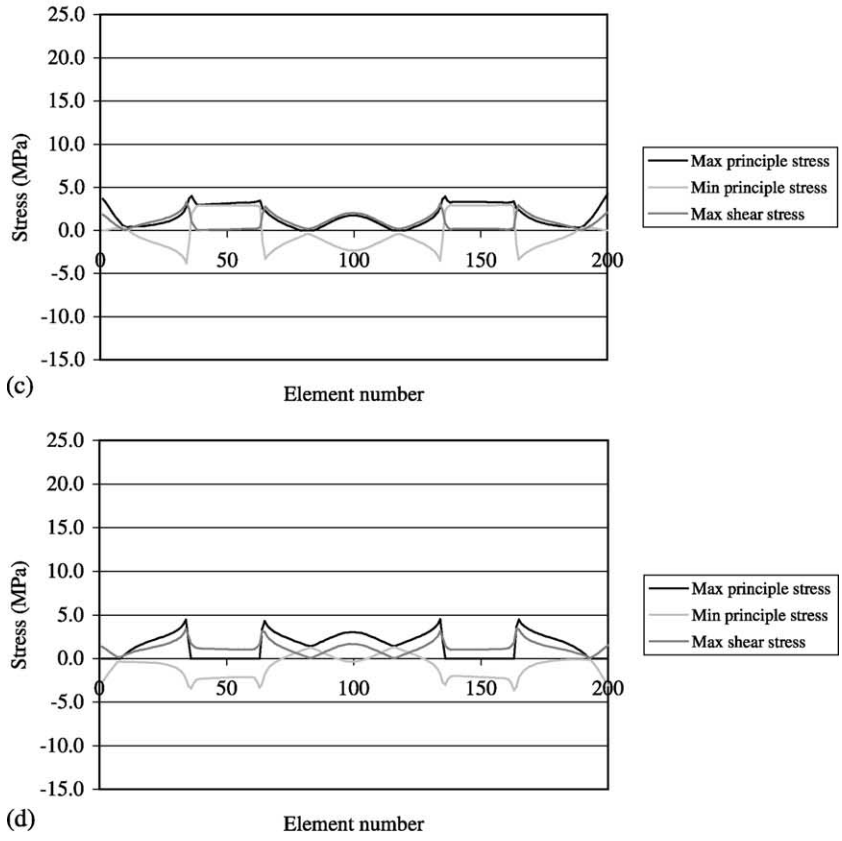

Fig. 2. Thermal stress field in specimens no. 1 and 2 at $\Delta T = 100$ °C. (a) Principal stresses in specimen no. 1 (CTE of inclusion $= 1.1 \times 10^{-6}$/°C); (b) principal stresses in specimen no. 2 (CTE of inclusion $= 0.9 \times 10^{-6}$/°C); (c) stresses distribution along mid-section *E–E* of specimen no. 1; (d) stresses distribution along mid-section *E–E* of specimen no. 2.

3.1.3. Effects of heterogeneity

Fig. 5a shows the thermal stress field of specimen no. 5 that consists of a heterogeneous matrix and inclusions. Comparing the stress distribution along the mid-section *E–E* of specimen no. 5 (Fig. 9) with that of specimen no. 1 with homogeneous phase materials (Fig. 2c), it is very

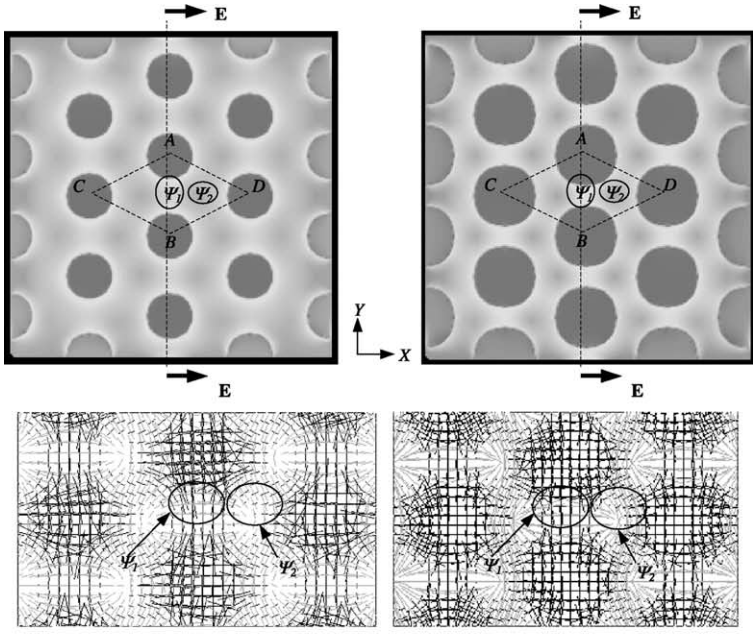

Light line indicates the minimum principal stress; dark line indicates the maximum principal stress

(a) (b)

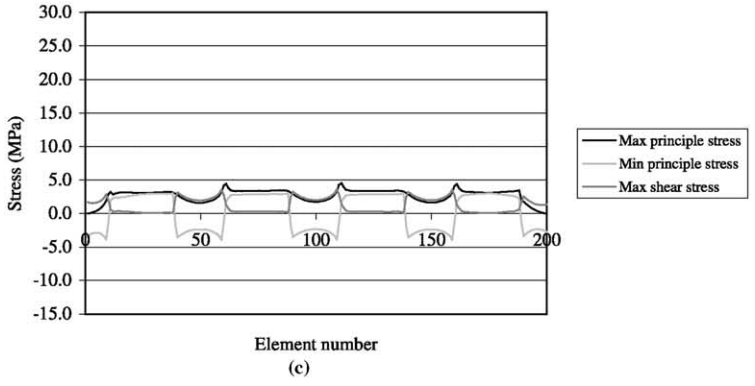

(c)

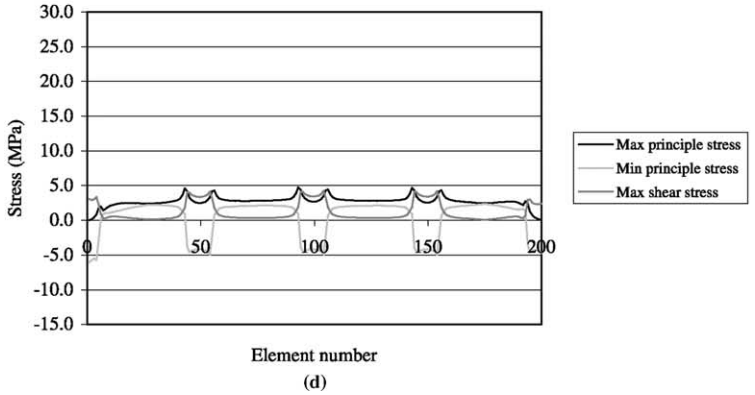

(d)

Fig. 3. Thermal stress field in specimens no. 1 and 3 at $\Delta T = 100$ °C. (a) Principal stresses in specimen no.1 (inclusion diameter = 15 mm); (b) principal stresses in specimen no. 3 (inclusion diameter = 20 mm); (c) stresses distribution along mid-section *E–E* of specimen no.1; (d) stresses distribution along mid-section *E–E* of specimen no. 3.

clear that the heterogeneity causes local fluctuation of stresses in the matrix and the inclusion even before crack initiates (see Fig. 9), even though their macroscopic thermal stress fields are identical from the statistical point of view. This leads to the early failure of the phase elements with a lower strength at lower elevated

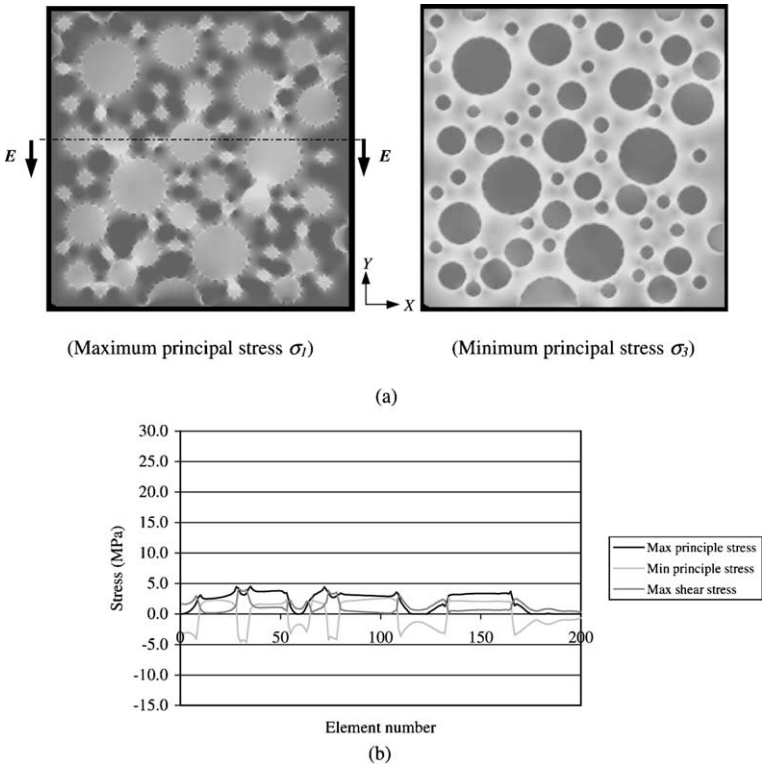

Fig. 4. Thermal stress field in specimens no. 4 at $\Delta T = 100$ °C. (a) Stress states; (b) stresses distribution along mid-section E–E of specimen no. 4.

temperatures (see Fig. 5b). With increasing temperatures, the number of the failed/broken elements also increased, and the extent of the stress fluctuation amplifies accordingly (see Fig. 9). For example, when the temperature is increased to 620 °C (see Fig. 5a and f), high stresses locate would locate at the tips of the irregular cracks, whose distributions are closely associated with the change in the heterogeneous mesostructure. The same phenomena are observed in specimens no. 6 and 7 which are heterogeneous phase materials (see Figs. 10 and 11).

3.1.4. Effects of size of multi-inclusions

In order to explain the effects of the distribution and size of the inclusions on the stress field, a composite material with multi-circular inclusions (specimen no. 4) with different diameters is numerically setup to calculate the thermal stress field (as shown in Fig. 4).

Although the macroscopic stress state in the composite is rather complex (see Fig. 4a), the critical zone of the stress concentration can be easily identified by measuring the distance between any given two inclusions. Fig. 4b clearly shows that the highest stress zones take place at the shortest distance between the two inclusions, and are not dictated by the diameter of the inclusions.

3.1.5. Effects of irregular inclusions

The thermal stress distributions of specimen no. 8 with multi-irregular-polygon inclusions are shown in Fig. 12.

It can be seen that as the matrix has a lower CTE than the inclusions, the stress states in the inclusions are in statistically hydrostatic compression, which are consistent with those observed in specimens no. 5 and 7. The sharp corners of the polygon inclusions induce the stress concentration. Such stresses around these inclusions look like the light luster emitting from a diamond (see Fig. 8). Attention should be drawn to the fact that the stress concentration is dominated by local notch effects in the matrix in the vicinity of the sharp corners of the inclusions.

3.2. Thermal fracture processes

3.2.1. Effects of thermal mismatch

Radial cracks are observed in specimens no. 5 and 7, in which the CTE of the inclusions is greater than that of the matrix (as shown in Figs. 5 and 7). Tangential cracks and inclusion cracks are found in specimen no. 6, in which the CTE of the inclusion is less than that of the matrix (see Fig. 6). The formations of typical crack patterns in multi-inclusion specimens are similar to those in the single-inclusion specimens reported in the companion Part I paper [11].

However, the alignments of the radial cracks in specimens no. 5 and 7 coincide with the shortest lines drawn between two neighboring inclusions. This observation cannot be found in the single-inclusion specimens.

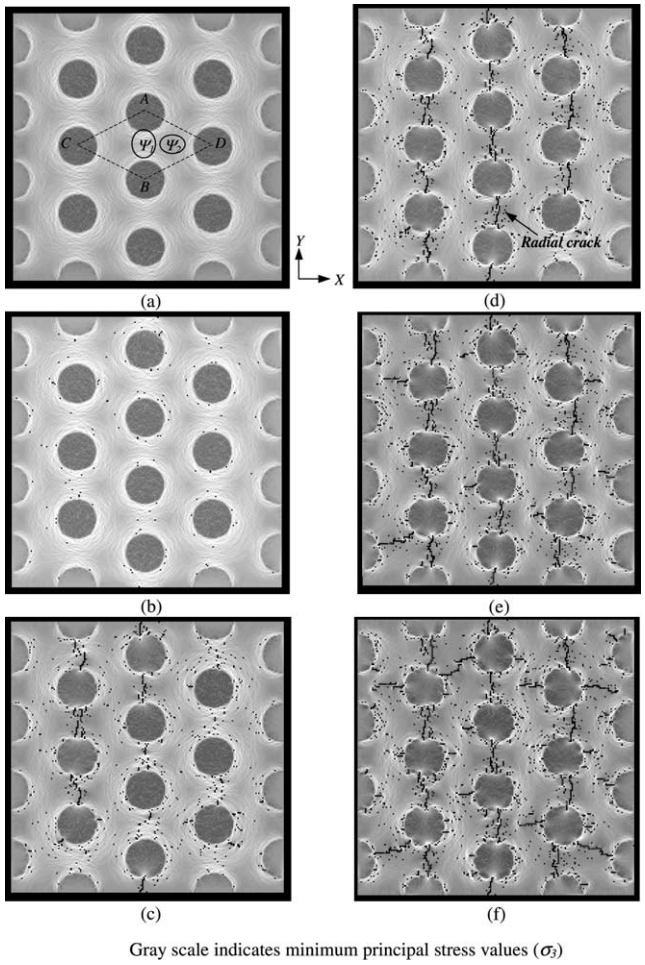

Fig. 5. Thermal stress field and cracking process of specimen no. 5 (inclusion diameter = 15 mm and CTE = 1.1×10^{-6}/°C). (a) $\Delta T = 20$ °C; (b) $\Delta T = 220$ °C; (c) $\Delta T = 370$ °C; (d) $\Delta T = 420$ °C; (e) $\Delta T = 520$ °C; (f) $\Delta T = 620$ °C.

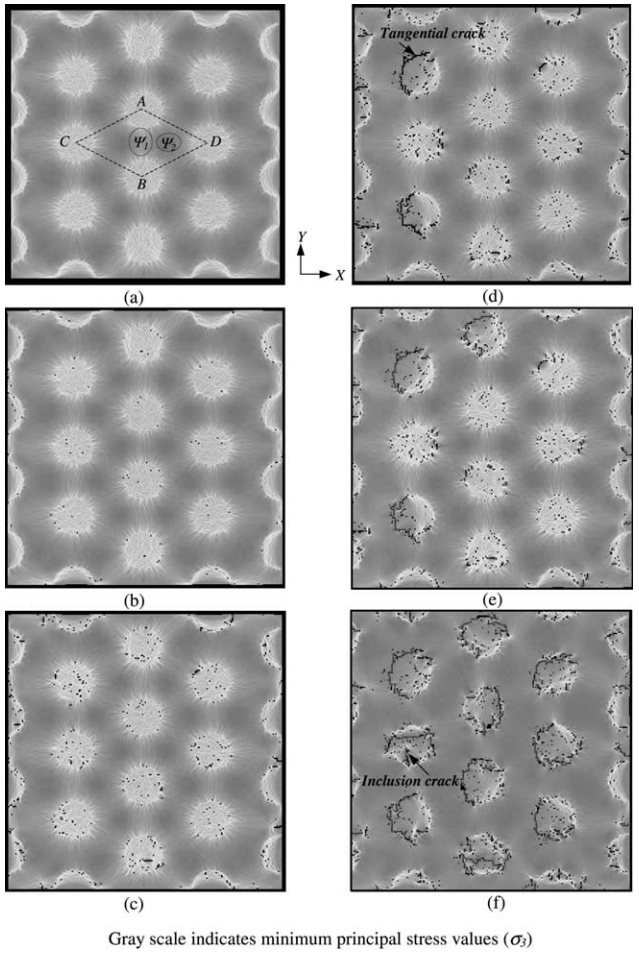

Fig. 6. Thermal stress field and cracking process of specimen no. 6 (inclusion diameter = 15 mm and CTE = 1.1×10^{-6}/°C). (a) $\Delta T = 20$ °C; (b) $\Delta T = 280$ °C; (c) $\Delta T = 430$ °C; (d) $\Delta T = 470$ °C; (e) $\Delta T = 480$ °C; (f) $\Delta T = 620$ °C.

3.2.2. Effects of size and arrangement of multi-inclusions

If the CTE of the inclusions is greater than that of the matrix, the cross-effect of stresses between the two neighboring inclusions makes the elements in sub-region Ψ_1 become more prone to failure. The onset of cracks is largely dependent on the size of the inclusions and the distance between any given two inclusions. For example, in specimen no. 5, majority of the early-formed broken matrix elements locate around the matrix-inclusion interfaces, from which radical cracks initiate and then propagate towards the neighboring inclusions along the shortest distance between the two neighboring inclusions (see Fig. 5). Consequently, most of the matrix cracks are along the Y-directional centre lines of the inclusions.

In specimen no. 7 with larger inclusions, early-formed broken matrix elements occur around the matrix-inclusion interfaces and also along the shortest paths between two neighboring inclusions. However, radical cracks initiate at the midways of the shortest paths, and then propagate towards the adjoining neighboring inclusions (see Fig. 7b). As the diameter of inclusions increases, the distance between ***A*** and ***C***, or ***C*** and ***B***, or ***B*** and ***D***, or ***D*** and ***A*** in specimen no. 7 reduces. Consequently, inclined cracks making an angle of about 30° to the X-axis, and as well as cracks along the Y-directional center lines of the inclusions are developed (see Fig. 7e and f).

However, when the CTE of the inclusions is less than that of the matrix (specimen no. 6), failed elements disorderly occur firstly in the inclusions (see Fig. 6c). With increasing temperatures, most of the cracks initiate and propagate along the interfacial zones between the matrix and the inclusion, where the tensile tangential stress is the highest (see Fig. 10). Cracks seldom initiate and spread in the cores of the inclusions unless under an unusual condition that the elastic modulus and the strength of matrix elements around the inclusions are much higher than those of the inclusion elements. As most of the damages (tangential cracks) occur around the interfacial zones and in the inclusions, the arrangement

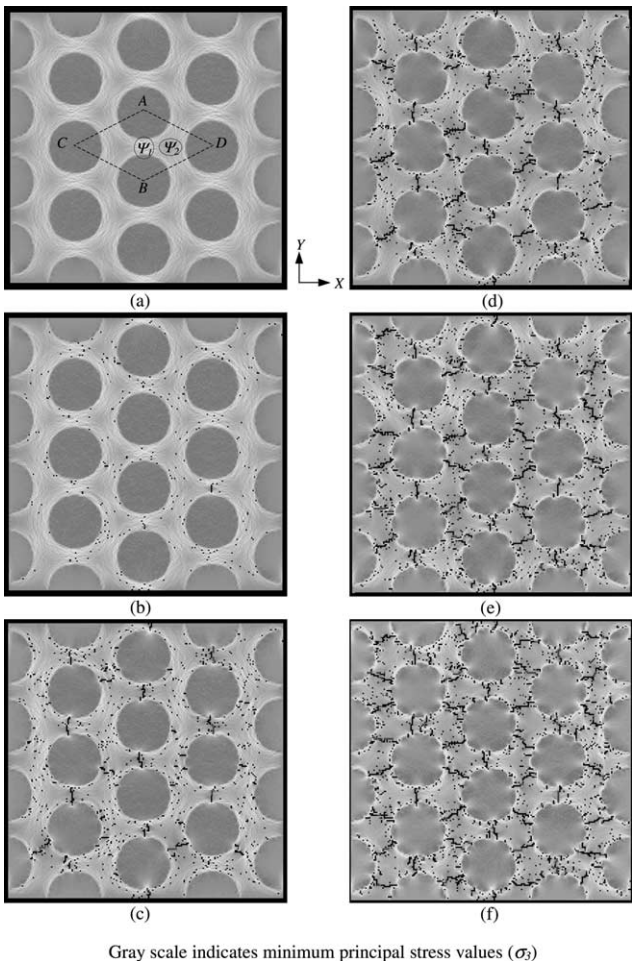

Fig. 7. Thermal stress field and cracking process of specimen no. 7 (inclusion diameter = 20 mm and CTE = 1.1×10^{-6}/°C). (a) $\Delta T = 20$ °C; (b) $\Delta T = 200$ °C; (c) $\Delta T = 320$ °C; (d) $\Delta T = 370$ °C; (e) $\Delta T = 470$ °C; (f) $\Delta T = 620$ °C.

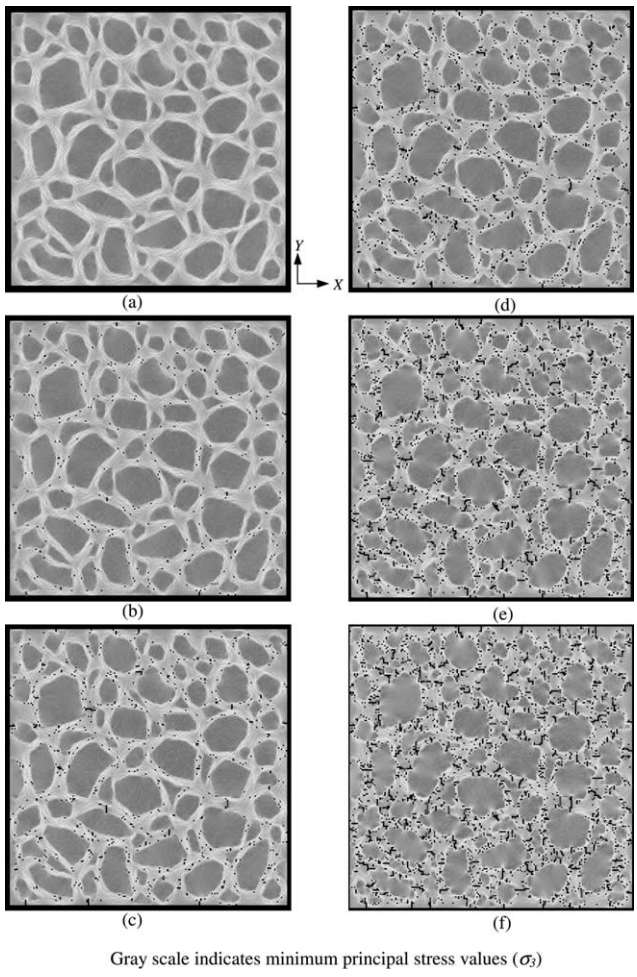

Fig. 8. Thermal stress field and cracking process of specimen no. 8 with multi-irregular inclusions (CTE = 1.1×10^{-6}/°C). (a) $\Delta T = 20$ °C; (b) $\Delta T = 200$ °C; (c) $\Delta T = 260$ °C; (d) $\Delta T = 320$ °C; (e) $\Delta T = 480$ °C; (f) $\Delta T = 620$ °C.

of inclusions has a less significant effect on the crack development. This phenomenon was confirmed in experimental studies by Cruz and Gillen. Investigations showed that the most serious disintegration of concrete in a fire is associated with the use of aggregates with large CTE [1]. This may be partly because joining the branch-orientated radical cracks in the matrix rather than by connecting the loop-orientated tangential cracks in the interfacial zones could form a potential plane of weakness across the specimen relatively easier.

3.2.3. Effects of heterogeneity

In the case of specimen no. 5, a diffused damage initially appears randomly in the whole region of the matrix at 220 °C (see Fig. 5b). It means that the failure of an element is dependent both on the thermal induced local stress and on the strength of the element. The strength distribution of the elements is mainly dependent on the heterogeneity at the meso-scale. Under the same stress field, the elements with a higher stress to the strength ratio have higher probabilities to fail than those with a lower ratio. Consequently, the shape of the crack path is irregular, rough and bifurcate; similar to the results reported in Part I of this paper [11].

Another interesting phenomenon can be observed from Figs. 5–8. The crack development is resisted by an inclusion with high elastic modulus and strength. When the tip of a radial crack touches an inclusion with a higher elastic modulus and strength, the inclusion obstructs the propagation of the radial crack. For example, in specimen no. 5, after the radial cracks coalesce between two-neighboring inclusions linking up in the Y-direction, they do not propagate when the tips of these cracks approach such an inclusion (see Fig. 5c–f). Instead, the radial cracks in the X-direction begin to initiate and propagate, since the stresses have been redistributed and transferred to the tips of these horizontal cracks. Thus the inclusion can play an important role to (i) resist further propagation of cracks, (ii) consume more energy required by failure, and (iii) dictate

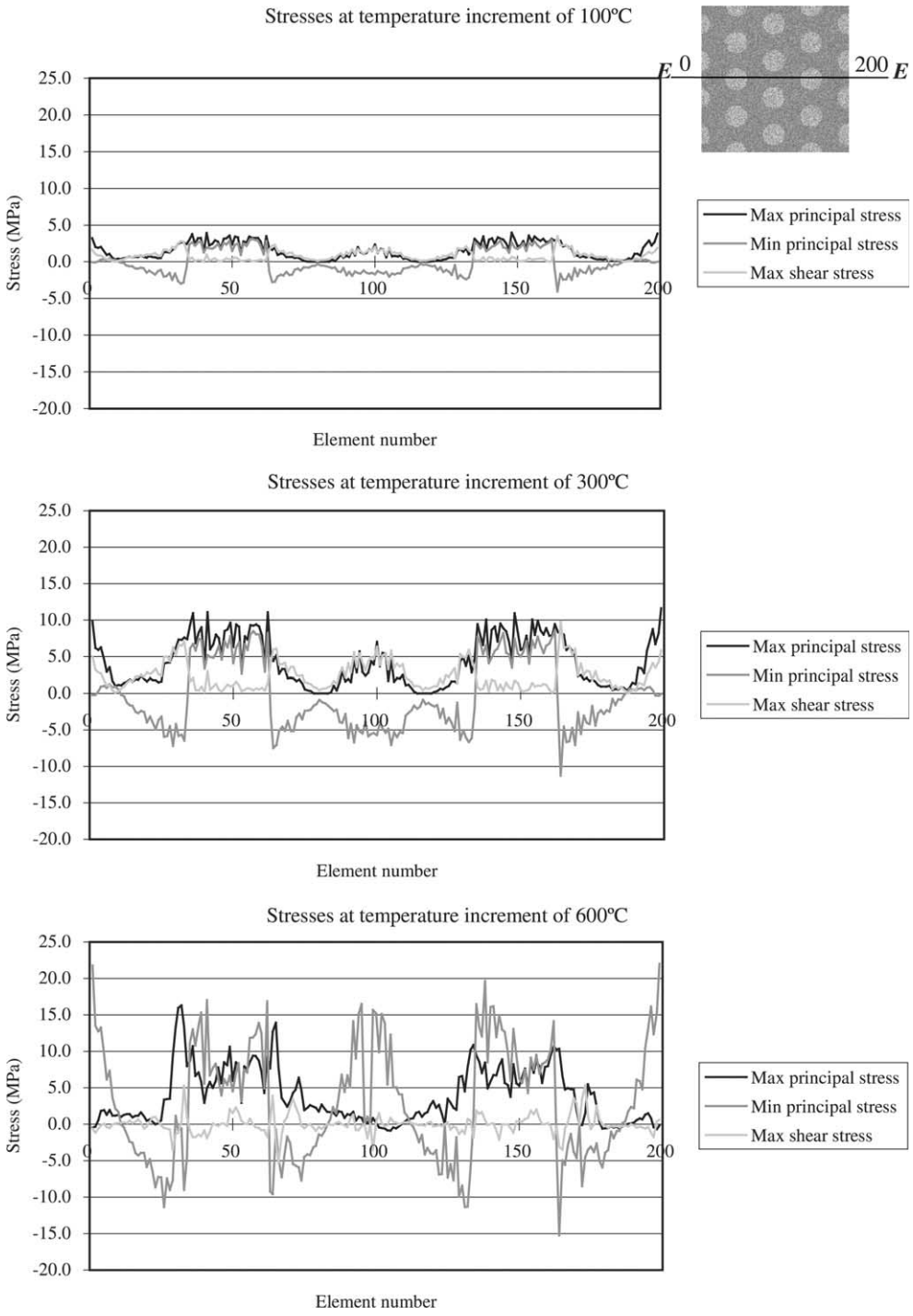

Fig. 9. Thermal stress distribution along mid-section E–E of specimen no. 5 (inclusion diameter = 15 mm and CTE = 1.1×10^{-6}/°C).

the redistribution of the stresses. These results are consistent with the conclusion drawn by Hansen and Kristensen [3] that a thermal crack probably travels in all directions in a mortar due to the presence of aggregates.

From the observation of the thermal fracture processes, it appears that heterogeneity can be used to interpret the randomization of crack origin and crack path. It can also be used to explain the local thermal fracture.

3.2.4. Thermal fracture evolution in composite with irregular inclusions

Specimens no. 5–7 are used to study the thermal fracture mechanism of a cement-based composite with multi-circular inclusions. As concrete is normally composed of irregular aggregates rather than circular aggregates, specimen no. 8 with multi-irregular-polygon inclusions is designed to study its thermal damage and fracture evolution.

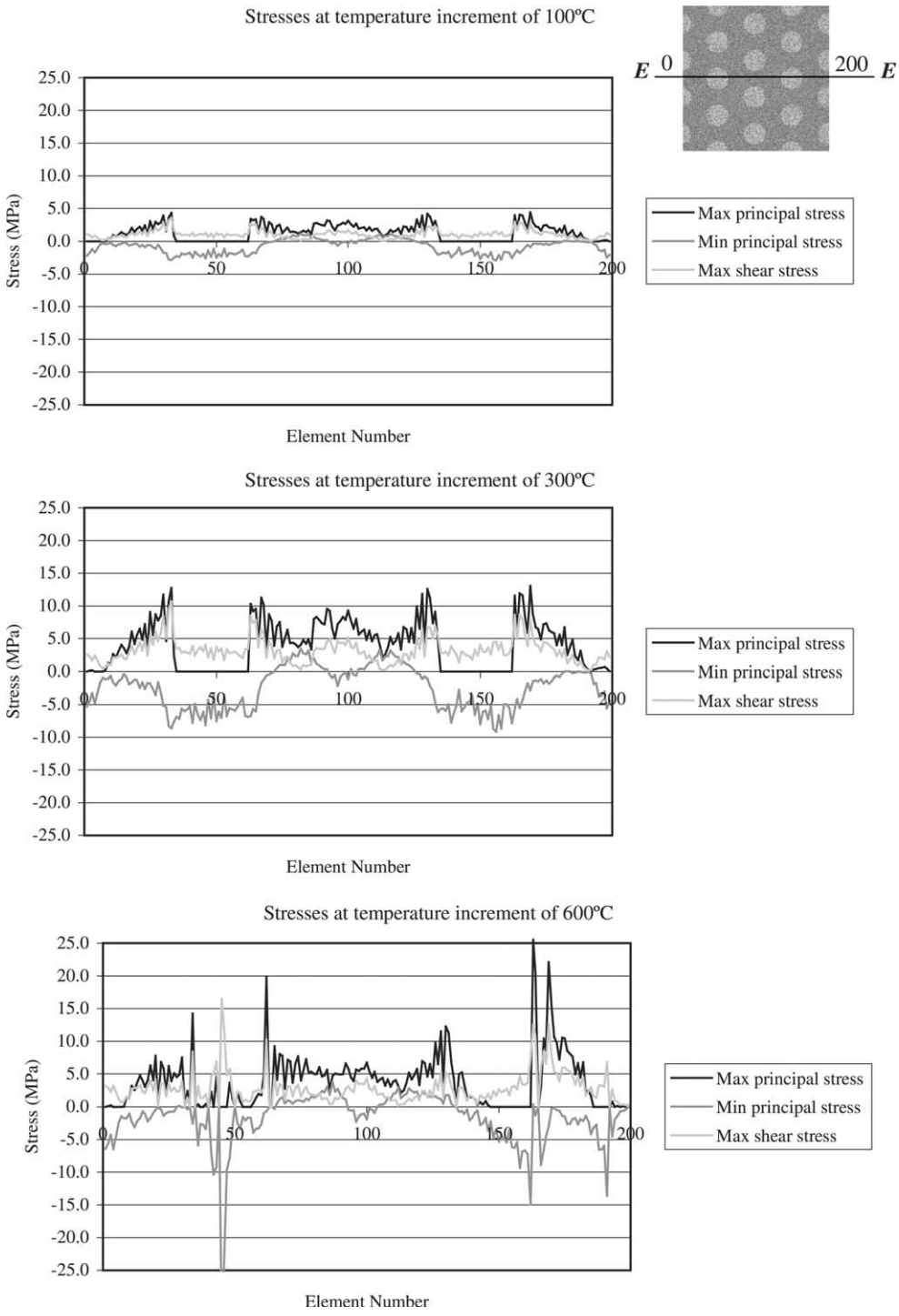

Fig. 10. Thermal stress distribution along mid-section *E–E* of specimen no. 6 (inclusion diameter = 15 mm and CTE = 0.9×10^{-6}/°C).

Since the CTE of the matrix is lower than that of the inclusions, the matrix is under bi-axial and the inclusions are under hydrostatic compressions, respectively. The damage initiates in the region near a sharp corner of a polygon inclusion or the area between the two inclusions having a shorter distance, as a result of high stress concentration. At a temperature of 250 °C, several vertical cracks propagate due to the stress concentration and the shortest distance between the corners of the two different inclusions. When the temperature reaches 260 °C, some horizontal cracks are formed. As the temperature further increases, more and more matrix elements get damaged, and the radical cracks propagate in all directions.

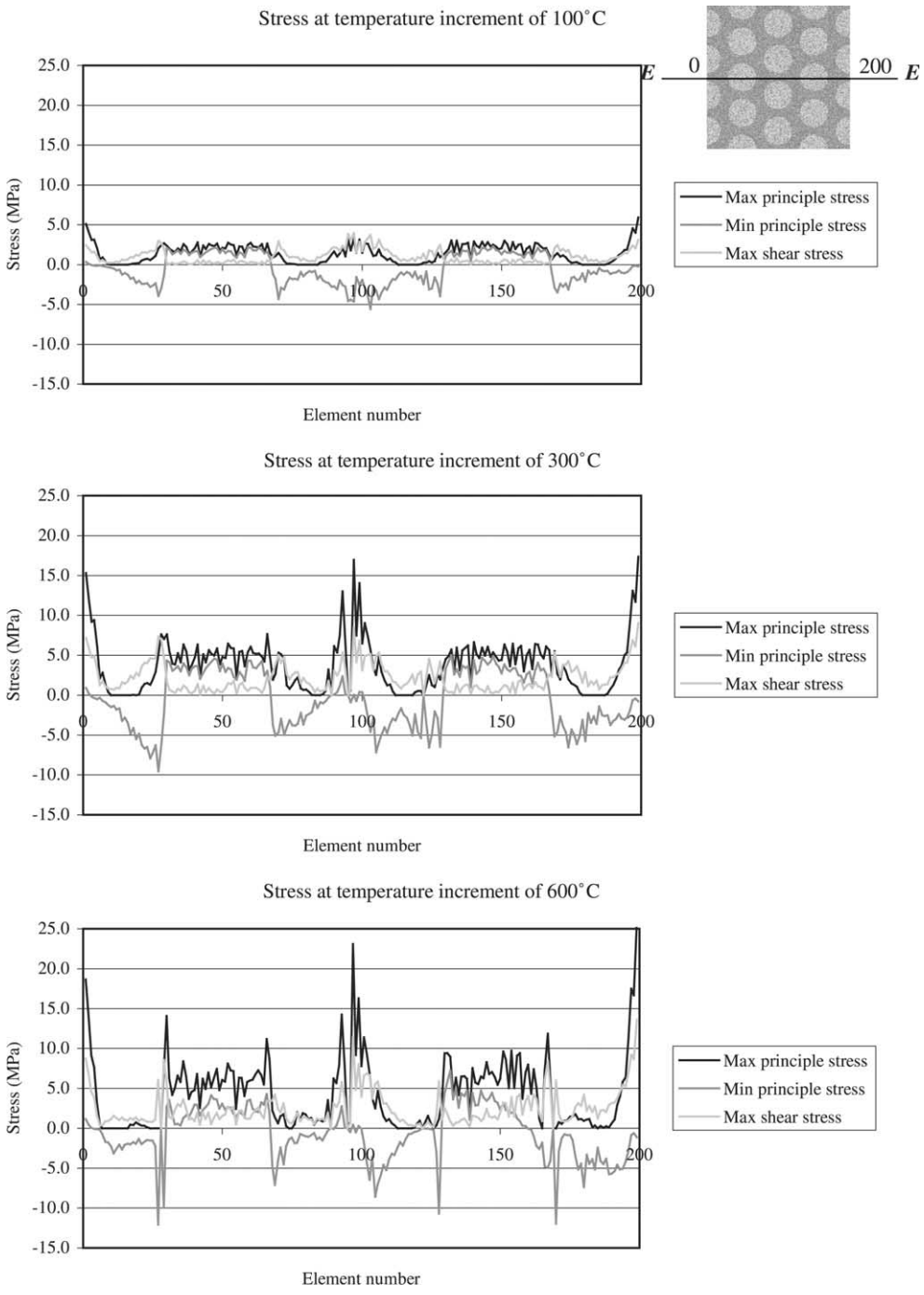

Fig. 11. Thermal stress distribution along mid-section *E–E* of specimen no. 7 (inclusion diameter = 20 mm and CTE = 1.1×10^{-6}/°C).

3.2.5. Effects of variable CTE

The numerical simulations indicate that there are two distinguished crack patterns: (a) radical cracks, and (b) tangential cracks and inclusion cracks, depending on either the CTE of the inclusion is constantly higher than that of the matrix or vice versa during the heating process.

In reality, the CTE of the aggregates and the cement paste in a concrete are temperature dependent. Within a lower temperature range, the CTE of the aggregates is generally smaller than that of the cement paste [12]. However, if the aggregates are produced from a parent rock with a high content of quartz (SiO_2), the commencement of the conversion of quartz at certain higher temperatures causes a substantial increase in CTE, as shown in Table 3 [13]. Moreover, cement pastes shrink, instead of expand, at a temperature greater than 100 °C, as a result of thermal decomposition of hydrates [12,14].

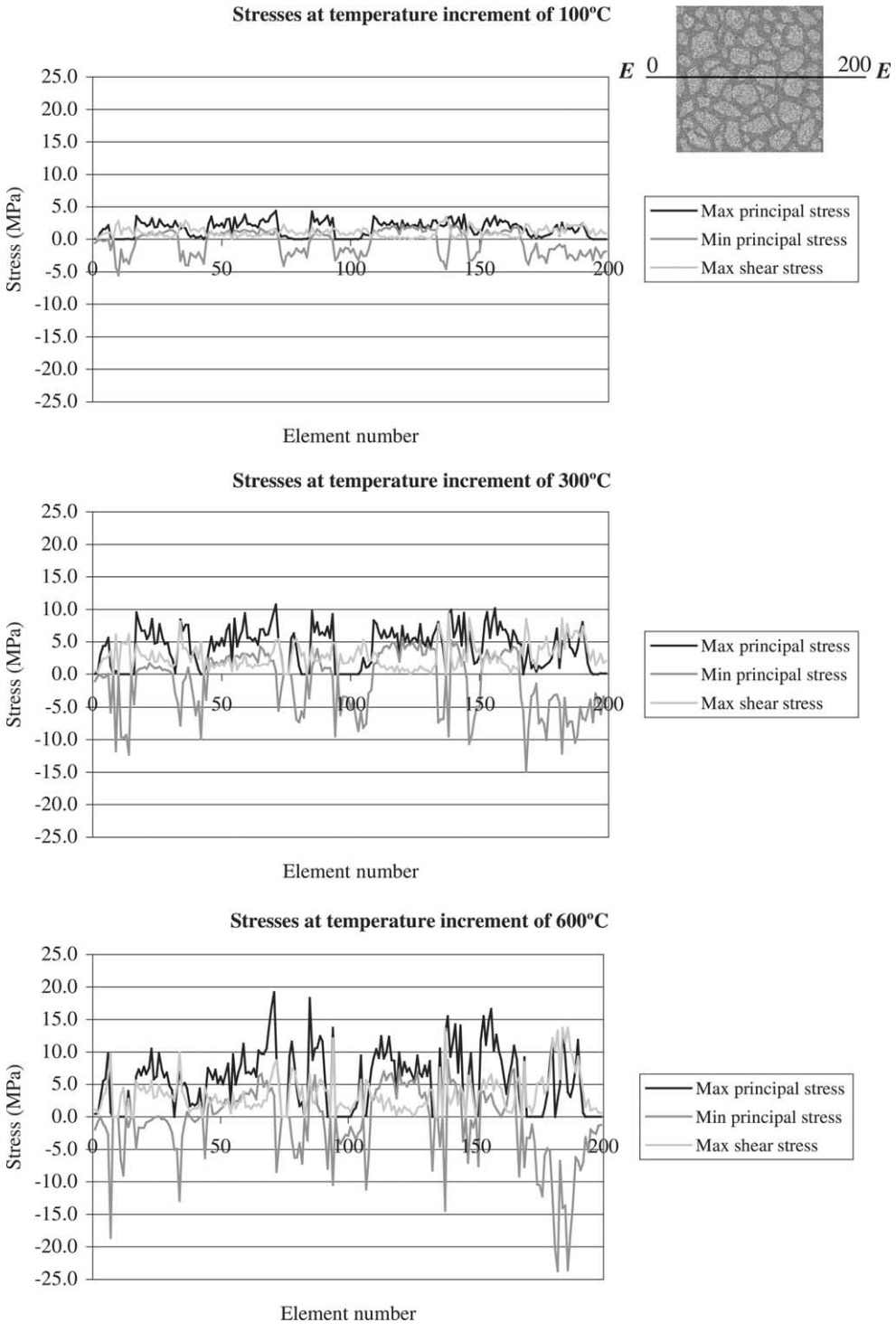

Fig. 12. Thermal stress distribution along mid-section *E–E* of specimen no. 8 with multiple irregular inclusions (CTE = 1.1×10^{-6}/°C).

Consequently, either radical cracks or tangential cracks plus inclusion cracks will form in concrete, depending whether the CTE of the aggregates is greater than that of the paste or not. When the temperature increases, such as above 530 °C, only radical cracks in the paste will be developed/extended, and they will dominate the thermal fracture process of the concrete.

4. Thermal damage in "good" concrete

It is recognized that a "good" concrete should be designed in such a way that every gap between the aggregates should be filled with smaller aggregates using a continuous granulometry, to minimize the use of the relatively expensive cement paste per unit volume of

Table 3
CTE in different ranges of temperatures [13]

Temperature range (°C)	Coefficient of thermal expansion ($\times 10^{-6}$/°C)			
	Sandstone (A)	Limestone (B)	Granite (C)	Anorthosite (D)
20–100	10.0	3.0	4.0	4.0
100–300	15.0	9.0	13.5	8.5
300–500	21.5	17.0	26.0	10.0
500–700	25.0	33.0	47.5	12.5

concrete. In such a way, the distance between the adjacent aggregates that is filled with a cement paste would be small. On the other hand, a ''bad'' concrete is the one with relatively wide gaps between the aggregates and filled with cement pastes. It can be predicted that the onset/quantity of thermal radical cracks in a ''good'' concrete is probably earlier/greater than those in a ''bad'' concrete because radical cracks are firstly initiated in regions between the two adjacent aggregates with a short distance apart. As the tip of a radical crack touches an aggregate, further propagation of the radical crack will be difficult unless the crack meanders around the aggregate. The latter requires more fracture energy. Therefore, upon an increasing temperature, the radical cracks in the ''good'' concrete would remain relatively short and tiny, but those in the ''bad'' concrete would further extend and grow into undesirable macro-cracks. Based on these considerations, the performance of a ''good'' concrete should be better than that of a ''bad'' concrete during fire attacks.

5. Conclusions

In this paper, a MTED model was used to numerically simulate the thermal stress field, and the cracking process of a cement-based multi-inclusions composite at elevated temperatures. The major findings from this study are summarized as follows.

1. The thermal stress field being studied is focused on the effects of thermal mismatch and the interaction of inclusions. If the CTE of the inclusions is greater than that of the surrounding matrix, the inclusions stress will be subject to hydrostatic compression and the matrix will be under bi-axially. Stress concentration in the matrix will occur in a region between any two-neighboring inclusions with the shortest distance apart, and at sharp corners of the inclusions. If the CTE of the inclusions are less than that of the matrix, the inclusions will be subject to bi-axial stress state and the matrix will be under hydrostatic compression. Critical stresses will occur in the inclusion-matrix interfacial zones.

2. The initiation and the path of cracks depend on the thermal mismatch and the matrix heterogeneity at meso-scale. When the CTE of the inclusions is larger than that of the matrix, the radical cracks will form in the matrix along the path between two neighboring inclusions that have the shortest distance apart. An increase in the inclusion diameter will change the location of the crack initiation and the direction of propagation of the radical cracks. As the tip of a radical crack touches an inclusion, further propagation of the crack is restrained. On the other hand, when the CTE of the inclusion is smaller than that of the matrix, tangential and inclusion cracks will form, and the associated thermal cracking process is not much affected by the arrangement of inclusions.

3. In concrete, the CTE of the aggregates and the cement paste are temperature dependent. Therefore, radical cracks, tangential cracks and inclusion cracks can form in the same concrete at different elevated temperatures. However, due to the shrinking character of the cement paste at higher elevated temperatures, it is expected that the radical crack development in the cement paste will control the thermal fracture process.

4. The initiation/quantity of the radical cracks in the cement paste of a ''good'' concrete in which every gap between the aggregates is filled with smaller aggregates using a continuous granulometry will be earlier/more than those in a ''bad'' concrete with relatively wide gaps between the aggregates. However, as the temperature increases, the radical cracks in the ''good'' concrete tend to remain short and tiny, while those in the ''bad'' concrete are more prone to extension and may develop into macro-cracks.

In this paper, the temperature-dependent properties (strength, elastic modulus and CTE) of each component material of the composite at high temperatures, which can substantially affect the thermal cracking process, have not been quantified. The authors are conducting further work in this direction.

Acknowledgements

The materials presented in this paper are some of the findings of the G-V848 research project entitled ''Thermal Stress and Associated Damage in Concrete at Elevated Temperatures'' of The Hong Kong Polytechnic University. The project is also partly supported by the NNSF of China (no. 50174013).

References

[1] Venecanin SD. Thermal incompatibility of concrete components and thermal properties of carbonate rocks. ACI Mater J 1990;87(6):602–7.
[2] Khoury A. Compressive strength of concrete at high temperatures: a reassessment. Mag Concr Res 1992;44(161):291–309.
[3] Kristensen L, Hansen TC. Cracks in concrete core due to fire or thermal heating shock. ACI Mater J 1994;91(5):453–9.
[4] Sumarac D, Krasulja M. Damage of plain concrete due to thermal incompatibility of its phases. Int J Damage Mech 1998;7:129–42.
[5] Hsueh CH, Becher PF, Sun EY. Analysis of thermal expansion behavior of intergranular two-phase composites. J Mater Sci 2001;36:255–61.
[6] Tijissens MGA, Sluys LJ, Giessen EVD. Simulation of fracture of cementitious composites with explicit modeling of microstructural features. Eng Fract Mech 2001;68:1245–63.
[7] Van Mier JGM. Fracture Processes of concrete: assessment of material parameters for fracture models. USA: CRC Press; 1997.
[8] Brandt AM. Cement-based composites: Materials, mechanical properties and performance. UK: E & FN Spon; 1995.
[9] Bažant ZP, Kaplan MF. Concrete at high temperatures: Material properties and mathematical models. UK: Longman House; 1996.
[10] Hsu Thomas TC. Mathematical analysis of shrinkage stresses in a model of hardened concrete. ACI J 1963:371–90.
[11] Fu YF, Wong YL, Tang CA, Poon CS. Thermal induced stress and associated cracking in cement-based composite at elevated temperatures—Part I: Thermal cracking around single inclusion. Cement Concr Compos, this volume. doi:10.1016/S0958-9465(03)00086-6.
[12] Neville AM. Properties of concrete. 3rd ed. UK: Longman House; 1993.
[13] Goltermann P. Mechanical predictions on concrete deterioration. Part 2: Classification of crack patterns. ACI Mater J 1995;92(1):58–63.
[14] Cruz CR, Gillen M. Thermal expansion of Portland cement paste, mortar and concrete at high temperatures. Fire Mater 1980;4(2):66–70.